Austrian Journal of Earth Sciences | Volume 103/1 | 29 - 42 | Vienna | 2010

# Walking through geologic history across a Neogene, incised anticline of the northern margin of the Tibetan plateau: review and synthesis

Andrea Brigitte RIESER[1)*], Franz NEUBAUER[1)], Yongjiang LIU[2)] & Johann GENSER[1)]

KEYWORDS

$^{40}Ar/^{39}Ar$ geochronology
stable isotope analysis
provenance analysis
Qaidam Basin
Altyn Tagh

[1)] Div. General Geology and Geodynamics, University of Salzburg, Hellbrunnerstrasse 34, 5020 Salzburg, Austria;

[2)] College of Earth Sciences, Jilin University, Changchun 130061, Jilin, China;

[*)] Corresponding author, andrea.rieser@nagra.ch

## Abstract

Climate and tectonics fundamentally influence the sedimentary environment, which is especially the case on the northernmost margin of the Tibetan plateau. There, the intramontane terrestrial Qaidam Basin records the regional geological history in its lacustrine, fluvial and alluvial sediments. In this contribution, we discuss source-sink relationships by interpreting the Eocene-Oligocene sedimentary succession of the Hongsanhan anticline along the northern margin of the Qaidam Basin, which formed during the Pliocene-Quaternary. The sedimentary succession shows a coarsening upward sequence reflecting the rapid uplift of the nearby Altyn Mountains. We review detrital white mica $^{40}Ar/^{39}Ar$ ages that yield information about hinterland geology and subsequent deep burial. Additionally our results of a detrital framework composition study reveal the mineralogy in the catchment area and demonstrate conditions during transport until final deposition. Moreover, we review stable isotope data that record the climatic and tectonic history as well as the depositional environment. We use this study on the Pliocene anticline structure on the northern margin of the Qaidam Basin, revealing sediments deposited between 50 – 26.5 Ma, to discuss advantages and limits of combining the aforementioned techniques.

Klima und Tektonik beeinflussen das sedimentäre Umfeld grundlegend, was vor allem am nordöstlichsten Rand des Tibetplateaus der Fall ist. Dort speichert das intramontane, terrestrische Qaidam Becken in seinen lakustrinen, fluvialen und alluvialen Sedimenten die regionale geologische Geschichte. In diesem Beitrag diskutieren wir den Zusammenhang von Herkunfts- und Ablagerungsraum, in dem wir die eozänen bis oligozänen Sedimentabfolgen der Hongsanhan-Antiklinale untersuchen, welche am Nordrand des Qaidam Beckens liegt und im Pliozän-Quartär entstand. Die Sedimentabfolge wird nach oben hin gröber, was die schnelle Hebung der nahen Altyn Berge widerspiegelt. Wir betrachten einerseits $^{40}Ar/^{39}Ar$ Alter von detritischen Hellglimmern, die Informationen über das Hinterland und die folgende Versenkung liefern, andererseits widerspiegeln die Resultate über die modale Zusammensetzung die Mineralogie im Einzugsgebiet und die Transportbedingungen bis zur endgültigen Ablagerung. Stabile Isotopen reflektieren sowohl die klimatische und tektonische Geschichte als auch die Bedingungen des Ablagerungsmilieus. Am Beispiel einer pliozänen Antiklinalstruktur am Nordrand des Qaidam Beckens, in welcher 50 bis 26.5 Ma alte Sedimente aufgeschlossen sind, diskutieren wir die Vorteile und Grenzen einer kombinierten Anwendung der oben erwähnten Methoden.

## 1. Introduction

It is widely accepted that surface uplift of the Himalayas and the Tibetan plateau changed the regional and even global climate (e.g. Ramstein et al., 1997), but how, when and to what extent is still highly debated. According to Raymo and Ruddiman (1992) the Tibetan uplift is one of the main driving forces behind Cenozoic climate change. Uplift of the southern Tibetan plateau has strengthened summer monsoon and brought wetter climates south of the Himalayas (Burbank et al., 2003; Sun and Wang, 2005); central Asia has become drier with the Himalayan range and the Tibetan plateau blocking moisture (Guo et al., 2002). The general Cenozoic climate of the Tibetan plateau is also considered arid with intervals of more humid conditions, especially in the Miocene (Wang et al., 1999). Such reconstructions are based on palaeoflora observations from Namling in southern Tibet (Spicer et al., 2003), pollen sequences (Wang et al., 1999) or distribution of sedimentary facies (Huang and Shao 1993). Dettman et al. (2003) and Garzione et al. (2004) performed detailed stable isotope studies on fluvial and lacustrine carbonates from the Linxia Basin, while Sun et al. (1999) and Graham et al. (2005) worked in the northern Qaidam Basin as well as the southern Tarim Basin. Recently, Sun et al. (2009) brought evidence – the presence of aeolian sediments – for the final onset of aridification in the Tarim Basin at ca. 7 Ma. A similar age for the onset of aridification can be expected, therefore, in the nearby Qaidam Basin.

If one analytical method alone does not yield results in the form of clear shifts or trends over a sequence of several samples, it might be helpful to apply other methods that require a different approach or independent methodologies. This is, for example, especially important in areas where the hinterland has variable crystallization and cooling ages, but is compositionally homogeneous. Clastic sediments record this source to sink pathway as well as preserve valuable information about the source region. Since source rocks might have been entirely eroded during subsequent tectonic events, it is fundamental to understand the nature and composition of their erosion

products. While sandstone composition mainly depends on the nature of the source area, factors like climate, weathering, erosion, relief, length of transport, sedimentation, burial and diagenesis can also alter the original source signature (Pettijohn et al., 1987; Johnsson, 1993; Fralick and Kronberg, 1997). Petrographic analysis, whole rock and mineral chemistry as well as radiometric dating can reveal the provenance and geodynamic development of sandstone-rich basin-fill successions.

$^{40}Ar/^{39}Ar$ thermochronology and other low-temperature thermochronometers (e.g. fission track and U-Th/He analysis) are powerful tools to evaluate erosion rates over geological time and to infer exhumation rates (e.g. Willett and Brandon, 2002; Brewer et al., 2003). Large-scale palaeogeographic relationships and tectonothermal cooling and denudation of orogens can be monitored with $^{40}Ar/^{39}Ar$ dating of detrital minerals such as white mica, biotite and K-feldspar (e.g. Copeland and Harrison, 1990; Najman et al., 1997). Different closure temperatures (ca. 425 °C for white mica (Harrison et al., 2009), ca. 300 °C for biotite, ca. 200 °C for K-feldspar (McDougall and Harrison, 1999) for slow cooling rates typical for regional-metamorphic areas make these K-bearing minerals suitable for estimation of exhumation rates in the source region. White mica usually yield well-defined plateau ages – provided they are not overprinted and reset, while feldspars are better suited for modelling cooling histories. In this study, we use white mica because of its abundance in the study area and its significance for tracing specific sources. In contrast to white mica, biotite has usually low chemical and mechanical resistance. Both biotite and white mica are well preserved in the Qaidam Basin due to the short transport distances as suspended load. The $^{40}Ar/^{39}Ar$ method allows straightforward comparison of both sedimentary rocks and the surrounding basement rocks and thus also recognition of changes in the hinterland. In addition, single grain total fusion ages can be verified by using the $^{40}Ar/^{39}Ar$ incremental heating method (for details, see Neubauer et al., 2007a).

In this study, we use the sedimentary succession exposed within the Hongsanhan (HSH) anticline to discuss: 1) the source-sink relationships, 2) distance to the basin margin and thus to the uplifting of the South Altyn Mountains and 3) expansion and shrinking of the Qaidam lake. In the three valleys of the HSH anticline we sampled carbonates and marls for stable isotope analyses, as well as (mica-bearing) sandstones for modal framework analysis and mineral dating with the $^{40}Ar/^{39}Ar$ technique. The temporal resolution is given by the vertical distance between the samples, which ranges from 10 cm in the lower fine-grained part up to 100 m in the coarser part at the top of the section. Discussion of the results is aided by the well-constrained geologic framework of the northern hinterland of the HSH.

## 2. Tectonical and geological setting of the Qaidam Basin

The Qaidam Basin developed as a triangular to rhomb-shaped intracontinental sedimentary basin through the interaction of climate and tectonics along the northern margin of the Tibetan plateau since the Eocene (Fig. 1). The region represents an area with moderate relief at ca. 2800 m between the high plateau with an elevation of 4000–5000 m and the Gobi and Tarim deserts at 1000 m elevation. The surrounding mountains, i.e. the Altyn Tagh in the north, the Qimantagh/Kunlun Mountains in the southwest and the Qilian Mountains in the northeast, reach heights in excess of 5000 m. All three mountain ranges contain dominant strike-slip fault systems, running more or less parallel to the ranges. Since at least Early Oligocene these ranges have completely enclosed the Qaidam Basin, which became dominated by internal drainage (Shi et al.,

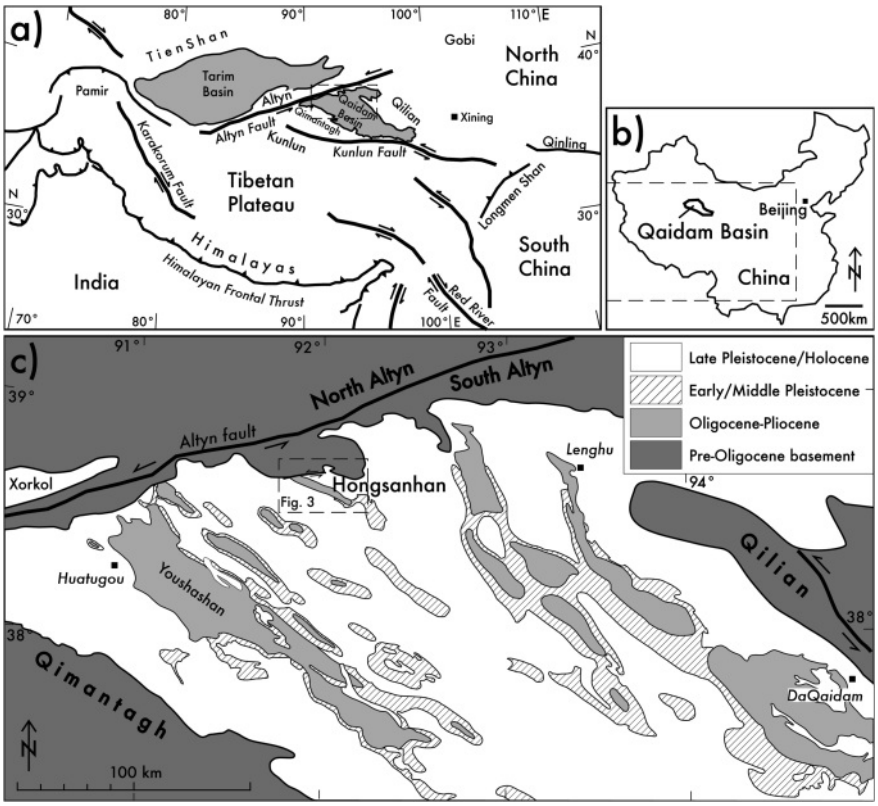


**Figure 1:** Simplified tectonic sketch map of the Himalaya-Tibet region (modified from Tapponnier et al., 2001). b) Position of the Qaidam Basin within China. c) Simplified geological map of the northwestern part of the Qaidam Basin with outlines of Pliocene fold structures.

2001; Zhu et al., 2006). During the Cenozoic, terrigenous sedimentary sequences were accumulated, from thicknesses of 3 km at the basin margin to about 10 km in the basin centre, and are divided into seven formations (Fig. 2; Yin et al., 2008b). Along the large crustal- to lithospheric scale sinistral strike-slip faults in the north and south of the basin, mountain ranges have been transported along the basin margins and therefore presenting continuously new material to erode within the catchment area, which is recorded in the sedimentary sequence. The initiation of displacement along the Altyn Fault was at about 50 – 45 Ma (Yin et al., 2007) and thus clearly influenced the facies pattern of our study area in the northern Qaidam Basin and also resulted in segmentation of the initial uniform basin. Strike-slip faults offer an explanation to why so much material has been accumulated in the basin, when apparent exhumation around is much less in the present-day catchment of the basin (Rieser et al., 2006; Wang et al., 2006). Because of this reason, Rieser et al. (2006) proposed a moving source, mainly the North Altyn Mountains, which were moving to the west with respect to the Qaidam block.

### 2.1 The Hongsanhan anticline

Our study area, the Hongsanhan (HSH) anticline, is situated at the northern margin of the Qaidam Basin (Fig. 3). On geological maps (Wang and Zhang, 1999) it is marked as Hongsanhan No. 1 anticline; for simplification we will use only HSH anticline.

The HSH anticline is separated from the South Altyn basement by an active sinistral strike-slip fault, the Datonggou fault (Genser et al., 2005). The HSH anticline strikes NW-SE, the northeastern limb is subvertical and partly overturned and its vergence is towards the South Altyn Mountains. In this respect, it is similar to other structures along the northern and northeastern margin of the Qaidam Basin, where mountain-facing anticlines are a characteristic feature and which are entirely different from other mountain front structures such as the Alps (Neubauer et al., 2007b; Yin et al., 2008a,b). Such structures at mountain fronts can be explained by a shallow basement beneath basin sediments, which acts like an indenter into the basin during shortening. Consequently, shortening of basin sedimentary succession is associated with surface uplift of adjacent basement, i.e. in the case of the HSH anticline by uplift of the South Altyn Mountains. The HSH anticline is one of several NW-trending fold structures (cf. Fig. 1c) that have formed in the Pliocene and Early Pleistocene (e.g. Song and Wang, 1993; Meyer et al., 1998). Unfortunately, no seismic section crossing the HSH exists, and consequently, the subsurface relationships of the basin fill are not constrained directly.

During the Eocene to Oligocene, the northwestern part of the Qaidam Basin was lower in elevation and largely covered by a lake (Huang et al., 1996). As the Altyn Mountains were below the snowline during the Cenozoic, no melt water was provided to the HSH area. Ostracods in the northern part of the Qaidam Basin therefore belong to only hypersaline species (Sun et al., 1999).

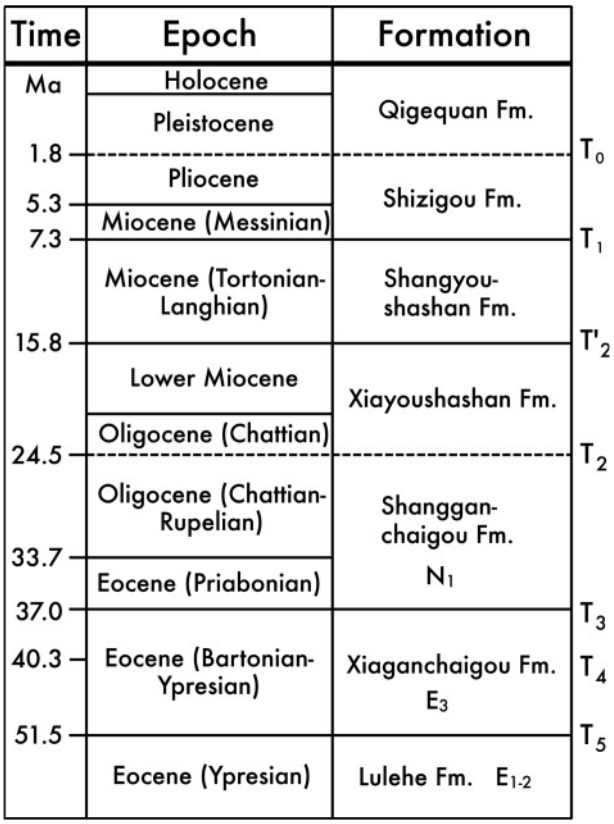


**Figure 2:** Cenozoic stratigraphy of the Qaidam Basin. Ages are based on Gradstein et al. (2004). $T_0$ to $T_5$ indicate seismic reflectors, which are correlated with biostratigraphically dated units from Qaidam drill cores, which mark formation boundaries.

The South Altyn Mountains, as the most likely source region exposed in the north of the HSH anticline, mainly expose a high-grade metamorphic terrain with migmatitic paragneisses, micaschists and amphibolites intruded by Lower Palaeozoic and subordinate Permian-Triassic granitoids (e.g. Jolivet et al., 1999; Gehrels et al., 2003b). As K-feldspar and apatite fission track data indicate, the South Altyn Mountains were finally ex-

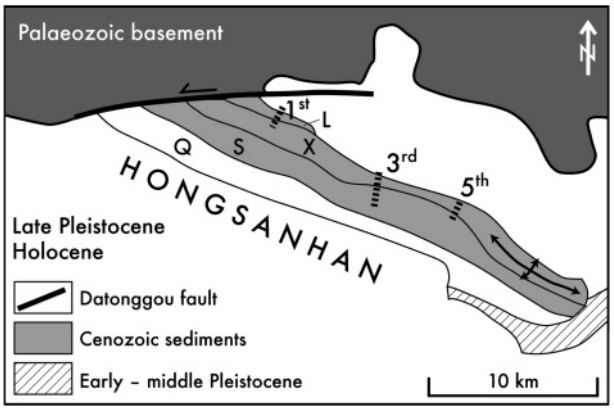


**Figure 3:** Detailed geological map of the Hongsanhan anticline at the northern margin of the Qaidam Basin. Dashed lines indicate the locations of the First, Third and Fifth High Peak Valleys, where this study was conducted. L: Lulehe Fm.; X: Xiaganchaigou Fm.; S: Shanggan-chaigou Fm.; Q: Qigequan Fm.

humed during Early Neogene.

Three sections have been studied in the HSH area including the so-called First, Third and Fifth High Peak Valleys (Fig. 3). The First High Peak Valley is close to the South Altyn Mountains and exposes the Lulehe Formation of mainly conglomerates. On its northern end, well-sorted, quartz-rich sandstones from the Lower Eocene Lulehe Formation (Fig. 4a) are exposed. They have been deposited at the basin margin probably at the outer rim of a delta. Above the red sandstones a thick sequence of conglomerates marks the formation boundary between the Lulehe and Xiaganchaigou formations (Fig. 4b). The boundary is defined by a thrust fault with small offset, indicated by fault and striae with gypsum fibres on the lower side of the conglomerates. The thrusting was most probably induced by folding of the anticline.

The Third High Peak Valley offers a ~1000 meter thick section through its southern limb (Fig. 5), covering almost 15 million years, i.e. from 40 to 26.5 Ma (Sun et al., 2005). The visible anticline core lies within the Eocene Xiaganchaigou Formation, where very fine-grained sediments dominate. A magnetostratigraphy study of the HSH Third Valley (Fig. 5; Sun et al., 2005) allows adequate time constraints in this particular section. Sediments in the Third Valley become coarser as the depositional environment evolves from deep lake (Fig. 4c) to fluvial to even alluvial (Fig. 5) as the Altyn Mountains continued to uplift. Within the overall coarsening upward trend, several fining upward cycles can be distinguished, starting with coarse sandstones or pebble conglomerates when lake level was low and grading into fine mudstones and marls with rising water. Marls occur particularly in horizons with abundant hydrocarbon source rocks (Ritts et al., 1999). At the top of the fining upward cycles carbonates were often deposited as a result of lake high-stands (Huang and Shao, 1993). The thickness of individual carbonate layers varies between a few and 20 cm, while some layers reach 1.5 m. The Quaternary alluvial gravel on top of the section is separated by an angular unconformity from the underlying Oligocene sandstones recording therefore, Miocene and/or Pliocene folding of the HSH anticline. The missing sediments are due to non-deposition and/or erosion as the northern basin was uplifted with uplift of the Altyn Mountains (Yin et al., 2008a,b). The northern basin margin uplifted and the lake withdrew towards southeast where the basin remained at relatively lower elevation.

In the following, we document some typical stages of the sedimentary facies based on the stratigraphic section shown in Figure 5. Representative facies of the whole section are shown

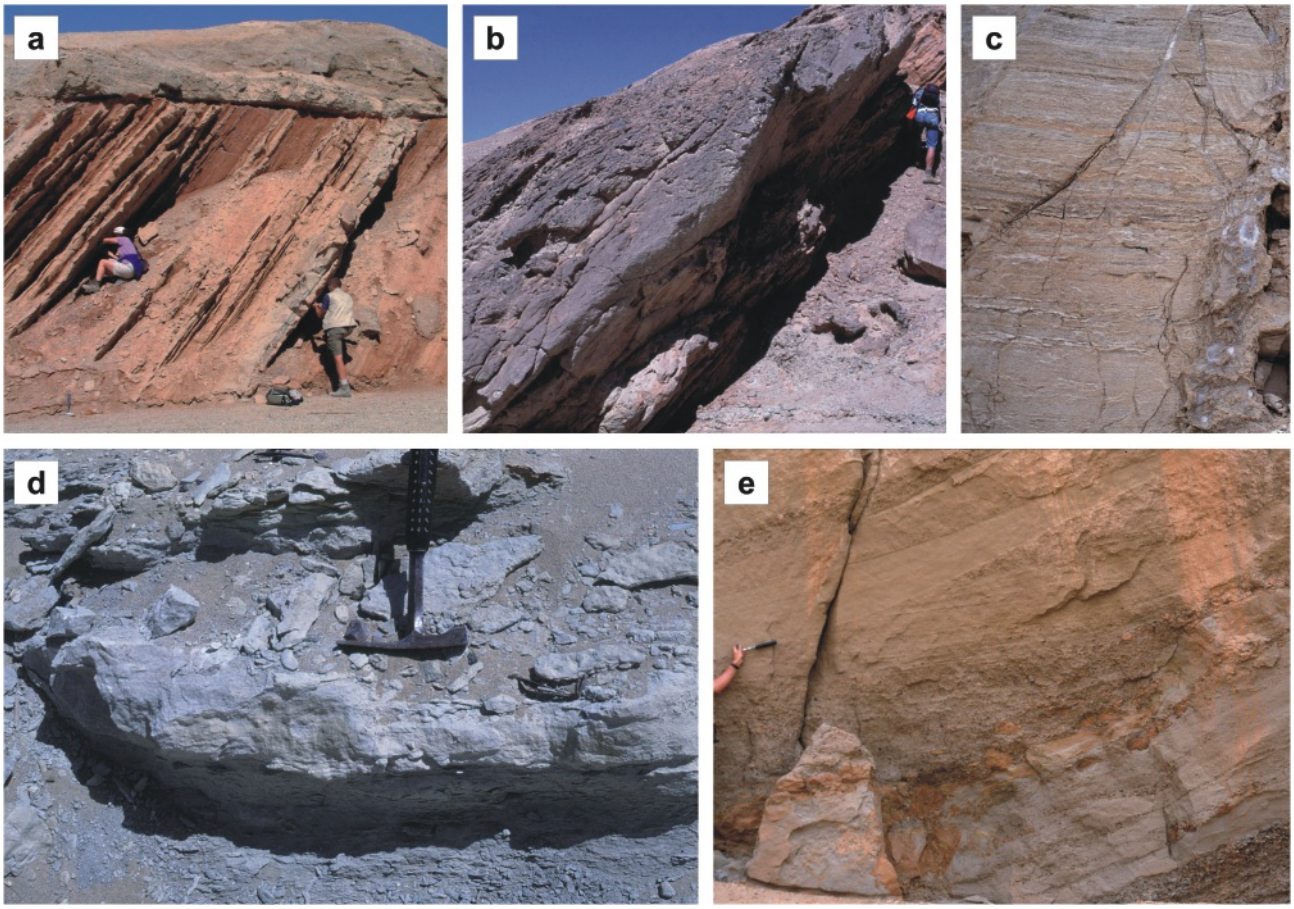


**Figure 4:** Representative examples of various facies types of the sedimentary succession exposed in the Hongsanhan anticline. a,b) Redbeds comprising conglomerates and sandstones of the Lulehe Fm., Hongsanhan First Valley. View is towards west. c) Well-laminated mudstones of the deep facies of the Xiaganchaigou Fm., Third Valley. Height of picture is 2.5 m. d) Limestone layer within siltstone of the Xiaganchaigou Fm. at the core of HSH anticline, Third Valley. e) Sandstone intercalation in deep lake facies in the Shangganchaigou Fm.

in Figure 4. After an initial stage of subsidence with redbeds comprising fluvial sandstones and conglomerates with subordinate siltstones (Lulehe Formation; Fig. 4a, b), the Xiaganchaigou and the lower part of the Shangganchaigou formations comprise mainly deep lake sediments (Fig. 4c, d) with mainly multi-coloured siltstone and marl and some limestone layers. The micritic-microsparitic carbonates of the Eocene Xiaganchaigou Formation of the Third High Peak Valley are within siltstones and are greenish-bluish (Fig. 4d) or beige and often marly and they are softer than the carbonates in the Fifth High Peak Valley, which lies 8 km further to the east. Stratigraphically upwards, the upper part of the Shangganchaigou Formation gradually shifts, starting at ca. 29 – 30 Ma (Sun et al. 2005), to a higher abundance of thick packages of coarse-grained sandstones (Fig. 4e) representing a coarsening upward cycle. Above an angular unconformity, the subsequent Qigequan Formation is characterized by thick terrestrial conglomerates and coarse-grained sandstones. These relationships are interpreted to monitor the surface uplift of the South Altyn Mountains between ca. 30–29 and 26 Ma superimposed by the local shrinking and migration to the southeast of the Qaidam lake. The increasing topography documented within the coarsening upward cycle is consistent with evidence of exhumation of South Altyn Mountains recorded by apatite fission track ages, which range from 19 ± 1 to 83 ± 7 Ma (Sobel et al., 2001).

The Fifth Valley is distant to the South Altyn Mountains and exposes a section with mainly fine-grained sediments of the Xiaganchaigou Formation, which are in part stratigraphically deeper than the deepest level of the Third Valley. In the Fifth Valley the dark-grey or greyish-brown carbonates of the Xiaganchaigou Formation are more abundant than in the Third Valley, extremely hard and when freshly sampled they strongly smell of petroleum, representing, therefore, deposits of the anoxic basin center facies. In the whole Fifth Valley, and in Oligocene time in the Third Valley as well, limestones are dominating.

## 3. Methods

### 3.1 $^{40}Ar/^{39}Ar$ mineral dating

Standard laser-fusion $^{40}Ar/^{39}Ar$ age determination has been performed on three samples from the southern limb of the First High Peak Valley. Sandstones were crushed and white mica was separated for $^{40}Ar/^{39}Ar$ mineral dating. Two samples are from the higher part of the Lulehe Formation and one from a large sandstone lense within the conglomerates at the lower boundary of the Xiaganchaigou Formation. From every sample 10 or 11 handpicked single white mica grains of 250–350 µm size have been measured at the ARGONAUT laboratory at Salzburg University, Austria with a laser-probe total fusion method. The complete procedure from preparation to measurement is described in detail in Rieser et al. (2006).

### 3.2 Modal framework analysis

In thin-sections of sandstones, 500 grains were counted in

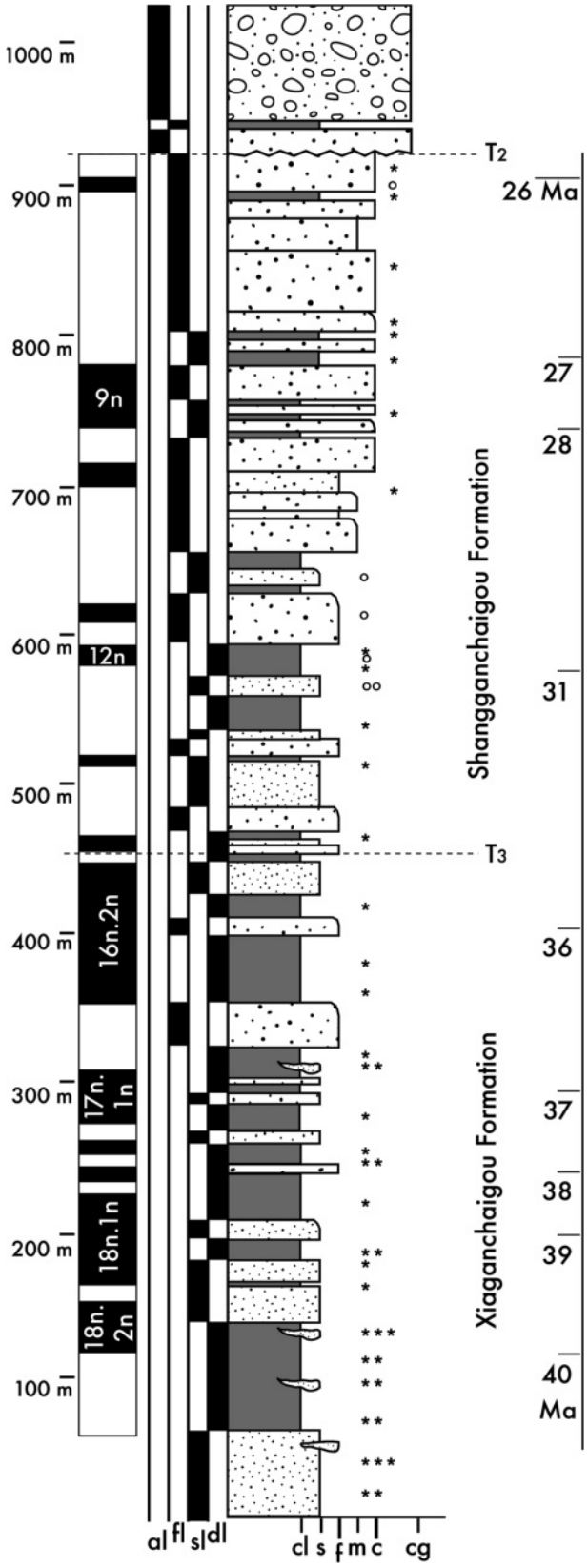


**Figure 5:** Lithostratigraphic column of the Hongsanhan Third High Peak Valley section (based on Ma, pers. comm. 2003) together with the magnetostratigraphy after Sun et al. (2005). $T_2$ and $T_3$ are seismic reflectors that define the formation boundaries. al – alluvial facies, fl – fluvial facies, sl – shallow lake facies, dl – deep lake facies, cl – clay, s – silt, f – fine sand, m – medium grained sand, c – coarse grained sand, cg – gravel. Stars indicate the location of carbonaceous samples for stable isotope analysis, open circles the location of sandstone samples used for point counting and or $^{40}Ar/^{39}Ar$ dating.

each using the Dickinson-Gazzi method (Dickinson, 1985) distinguishing framework constituents (0.063–2 mm) and cement or matrix. Framework mineral composition allows the ability to distinguish several provenance settings (e.g. Dickinson, 1985). Based on Dickinson and Suczek (1979) and Dickinson (1985) modal analysis of framework constituents includes: monocrystalline quartz ($Q_m$), polycrystalline quartz ($Q_p$), plagioclase and K-feldspar, constituting together feldspar (F) also including microcline, lithic sedimentary and metasedimentary clasts ($L_s$) and lithic volcanic clasts ($L_v$). $L_s$ and $L_v$ constitute the lithic clastics (L) and together with $Q_p$ the total lithic clastics ($L_t$). $Q_m$ and $Q_p$ make the total quartz ($Q_t$). Furthermore we distinguished detrital white mica, biotite and carbonates. Opaques, heavy minerals, chlorite and amphiboles were combined for this study. Feldspars were, regardless of their degree of alteration, classified as such if they could be positively identified due to remnant shapes of uniform extinction.

### 3.3 Oxygen and carbon stable isotope analyses

Well-homogenized whole rock samples of carbonates and marls were measured in an automatic Kiel II preparation line and a Finnigan MAT Delta Plus mass spectrometer at the Institute of Geology and Palaentology at the University of Graz, Austria (for details, see Rieser et al., 2009). For accuracy control NBS-19 and an internal laboratory standard were continuously analysed. The standard deviation is ±0.1‰ for $\delta^{18}O$ and ±0.06‰ for $\delta^{13}C$. All results are reported in the δ-notation in per mil (‰) relative to the Peedee belemnite standard (PDB).

## 4. Results

All the data used in this paper are published in other papers with specific foci in the context of the entire Qaidam Basin. The $^{40}Ar/^{39}Ar$ data of detrital white mica can be found in Rieser et al. (2006, 2007), the compositional data of sandstones in Rieser et al. (2005) and the stable isotope data in Rieser et al. (2009), respectively. The data are summarized and shown in Table 1 and Figure 6 ($^{40}Ar/^{39}Ar$ ages), Table 2 and Figure 7 (modal framework analysis) and Figure 8 (stable isotope analyses), respectively.

| Sample | Fm. | Qm | F | Lt | Qt | F | L |
|---|---|---|---|---|---|---|---|
| QA-189C | S | 72 | 19 | 9 | 74 | 19 | 7 |
| QA-186I | S | 64 | 21 | 15 | 67 | 21 | 12 |
| QA-186G | S | 52 | 31 | 17 | 54 | 31 | 15 |
| QA-186D | S | 57 | 31 | 12 | 59 | 31 | 10 |
| QA-186C | S | 62 | 29 | 9 | 62 | 29 | 9 |
| QA-186B | S | 47 | 35 | 18 | 49 | 35 | 16 |
| QA-130B | X | 57 | 21 | 22 | 59 | 21 | 20 |
| QA-133B | X | 56 | 31 | 13 | 57 | 31 | 12 |
| QA-133C | X | 59 | 28 | 13 | 61 | 28 | 11 |
| QA-133A | L | 59 | 22 | 19 | 62 | 22 | 16 |
| QA-132A | L | 70 | 13 | 17 | 76 | 13 | 11 |

**Table 2:** Normalized sandstone composition data from the Hongsanhan anticline. Samples are in stratigraphic order. The complete data can be found in Rieser et al. (2005). S: Shangganchaigou Fm.; X: Xiaganchaigou Fm.; L: Lulehe Fm.

In sample 132A (Lulehe Fm.) the age interval of 420–440 Ma clearly dominates (Fig. 6), while sample 133A (Lulehe Fm.) shows a concentration of 320–380 Ma ages and only a single Early Palaeozoic age. Sample 133C (Xiaganchaigou Fm.) contains three Early Palaeozoic ages (488–522 Ma) and some younger scattered ages.

The detrital mode data of sandstones (Fig. 7) can be characterized as those rocks, which plot in the recycled orogenic field ($Q_t$-F-L) and the transitional continental and mixed zone ($Q_m$-F-$L_t$). There is no visible difference in modal framework composition between the three investigated formations.

Stable isotope data in Figure 8 show large variations for $\delta^{13}C$ values in the Xiaganchaigou Formation of the Third Valley between –5.5 and –0.3‰ with several rapid positive excursions, while samples from the Shangganchaigou Formation vary less between –2.7 and –1.6‰. The samples from the Fifth Valley section yield lighter isotopic values between –5.5 and –3.7‰ with one excursion to –1.4‰. The $\delta^{18}O$ values for the Third

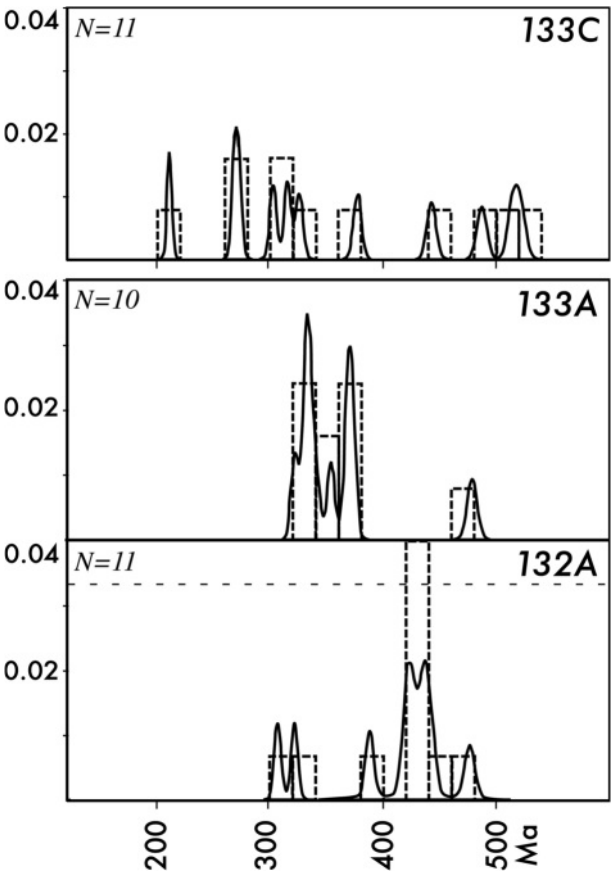


**Figure 6:** $^{40}Ar/^{39}Ar$ ages of white mica total-fusion analyses from the Hongsanhan First High Peak Valley (for details, see Rieser et al., 2006). Dashed columns give the number of measured grains between 0 and 5. In sample 132A 6 grains show the same age (wide-spaced dashed line marks 5 samples). Solid lines show the cumulative probability. Samples 132A and 133A are from the Lulehe Fm., sample 133C is from Xiaganchaigou Fm.

Valley range between –8.4 and –5.2‰ with several positive excursions in the lower part. In the limestone dominated part in the Shangganchaigou Formation values vary within two per mil (–8.4 to –6.6‰). In the Fifth Valley $\delta^{18}O$ values range from –3.9 to –7.5‰.

## 5. Discussion

The Hongsanhan area derived its detrital material generally from the Altyn Mountains in the north. In the Altyn Mountains, ages in the 350–450 Ma range are well-documented in the metamorphic and granitic basement (Fig. 9). In particular, this age group, interpreted as cooling ages, dominates the basement rocks of the Xorkol area (Jolivet et al., 1999; Sobel et al., 2001; Gehrels et al., 2003a), which lies on the northern side of the Altyn fault, northeast of the HSH anticline. Our analyzed detrital mica grains have preserved similar cooling ages (cooling below ca. 425 °C) with little to no indication of subsequent reheating above the minerals' closure temperatures. When a mineral is heated above closure temperature it starts to lose argon. In such would be the case, stepwise-heating analysis would yield a staircase-pattern with young ages at low experi-mental temperatures and older, possibly original, ages in high temperature steps. Such overprint can happen during deep burial or thrusting. In another study (Rieser et al., 2006, 2007) we concluded through our single-grain step heating experiments that Qaidam samples show no significant tectonothermal overprint after deposition and therefore simple single-stage tectonothermal, likely cooling histories in the respective source regions.

| $^{36}Ar/^{39}Ar$ meas. | $^{36}Ar/^{39}Ar$ 1-sigma abs. | $^{37}Ar/^{39}Ar$ corr. | $^{37}Ar/^{39}Ar$ 1-sigma abs. | $^{40}Ar/^{39}Ar$ meas. | $^{40}Ar/^{39}Ar$ 1-sigma abs. | $\%^{40}Ar^*$ | age [Ma] | +/- [Ma] 1-sigma abs. |
|---|---|---|---|---|---|---|---|---|
| QA-133C-01 with J=0.01862 | | | | | | Xiaganchaigou Fm | | |
| 0.00048 | 0.00003 | 0.00052 | 0.00002 | 10.411 | 0.008 | 98.6 | 315.2 | 3.0 |
| 0.00028 | 0.00002 | 0.00113 | 0.00002 | 15.044 | 0.007 | 99.4 | 442.9 | 4.0 |
| 0.00323 | 0.00020 | 0.02698 | 0.00019 | 11.591 | 0.059 | 91.8 | 325.6 | 3.5 |
| 0.00109 | 0.00006 | 0.00819 | 0.00006 | 9.074 | 0.017 | 96.4 | 271.9 | 2.6 |
| 0.00038 | 0.00007 | 0.00043 | 0.00007 | 12.625 | 0.020 | 99.1 | 377.4 | 3.5 |
| 0.00039 | 0.00005 | 0.00007 | 0.00005 | 17.873 | 0.016 | 99.3 | 515.0 | 4.6 |
| 0.00026 | 0.00006 | 0.00010 | 0.00005 | 6.732 | 0.018 | 98.8 | 210.3 | 2.1 |
| 0.00029 | 0.00007 | 0.00064 | 0.00008 | 8.700 | 0.022 | 99.0 | 268.0 | 2.6 |
| 0.02734 | 0.00013 | 0.00229 | 0.00007 | 17.903 | 0.039 | 54.9 | 302.6 | 3.0 |
| 0.00030 | 0.00006 | 0.00197 | 0.00006 | 16.772 | 0.017 | 99.5 | 487.6 | 4.4 |
| 0.00167 | 0.00018 | 0.01721 | 0.00019 | 18.524 | 0.054 | 97.3 | 521.9 | 4.8 |
| QA-133A-01 with J=0.01862 | | | | | | Lulehe Fm | | |
| 0.00018 | 0.00004 | 0.00004 | 0.00003 | 16.392 | 0.011 | 99.7 | 479.2 | 4.3 |
| 0.00108 | 0.00009 | 0.00102 | 0.00007 | 11.251 | 0.025 | 97.2 | 334.3 | 3.2 |
| 0.00065 | 0.00006 | 0.00099 | 0.00005 | 12.353 | 0.017 | 98.5 | 368.3 | 3.4 |
| 0.00461 | 0.00009 | 0.00267 | 0.00007 | 11.856 | 0.026 | 88.5 | 322.0 | 3.1 |
| 0.00299 | 0.00006 | 0.00298 | 0.00004 | 12.526 | 0.017 | 92.9 | 354.0 | 3.3 |
| 0.02466 | 0.00016 | 0.00153 | 0.00009 | 18.095 | 0.047 | 59.7 | 330.8 | 3.4 |
| 0.00304 | 0.00014 | 0.00097 | 0.00013 | 12.060 | 0.042 | 92.5 | 340.6 | 3.4 |
| 0.00130 | 0.00004 | 0.00005 | 0.00004 | 11.276 | 0.012 | 96.6 | 333.2 | 3.1 |
| 0.00019 | 0.00006 | 0.00026 | 0.00005 | 12.386 | 0.018 | 99.6 | 372.9 | 3.5 |
| 0.00071 | 0.00008 | 0.00015 | 0.00007 | 12.478 | 0.023 | 98.3 | 371.2 | 3.5 |
| QA-132A-01 with J=0.01855 | | | | | | Lulehe Fm | | |
| 0.03214 | 0.00532 | 0.05867 | 0.00550 | 23.780 | 1.582 | 60.1 | 424.0 | 42.0 |
| 0.00031 | 0.00007 | 0.00082 | 0.00007 | 14.528 | 0.020 | 99.4 | 428.1 | 3.9 |
| 0.00171 | 0.00006 | 0.00099 | 0.00005 | 13.443 | 0.019 | 96.2 | 388.1 | 3.6 |
| 0.00521 | 0.00023 | 0.00498 | 0.00017 | 15.679 | 0.067 | 90.2 | 420.3 | 4.2 |
| 0.00073 | 0.00006 | 0.00237 | 0.00005 | 10.733 | 0.018 | 98.0 | 321.5 | 3.1 |
| 0.00020 | 0.00016 | 0.00200 | 0.00013 | 16.373 | 0.046 | 99.6 | 476.9 | 4.5 |
| 0.00030 | 0.00006 | 0.00042 | 0.00005 | 14.787 | 0.018 | 99.4 | 435.0 | 4.0 |
| 0.00071 | 0.00009 | 0.00019 | 0.00007 | 15.006 | 0.026 | 98.6 | 437.6 | 4.0 |
| 0.00101 | 0.00009 | 0.00054 | 0.00007 | 15.298 | 0.027 | 98.0 | 442.9 | 4.1 |
| 0.00008 | 0.00012 | 0.00005 | 0.00011 | 10.012 | 0.037 | 99.8 | 306.7 | 3.1 |
| 0.00064 | 0.00010 | 0.00004 | 0.00008 | 14.432 | 0.029 | 98.7 | 422.9 | 3.9 |

**Table 1:** $^{40}Ar/^{39}Ar$ results from total-fusion analyses on detrital white mica single-grains from the Hongsanhan First high Peak Valley.

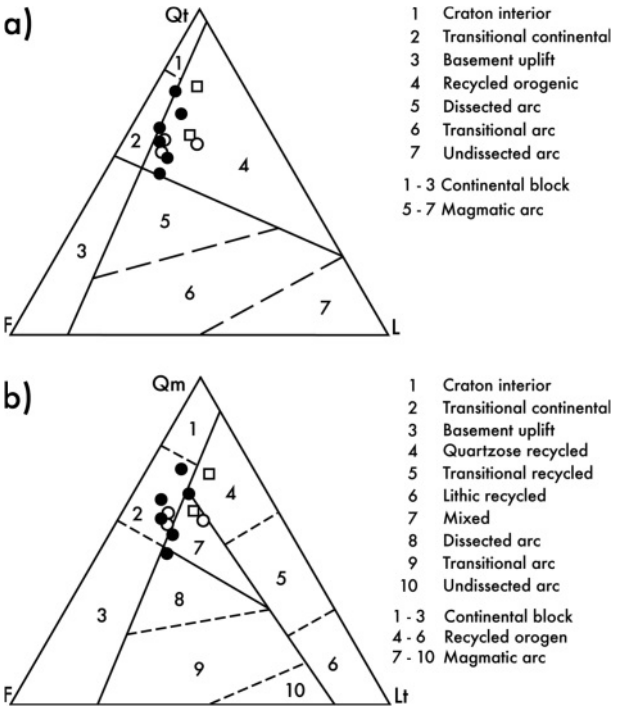


**Figure 7:** Triangular discrimination diagrams of sandstones from the Hongsanhan anticline. Black dots: Shangganchaigou Fm.; open circles: Xiaganchaigou Fm.; open squares: Lulehe Fm. a) Framework-grain assemblage Qt-F-L. b) Framework-grain assemblage Qm-F-Lt. Fields of various tectonic settings are from Dickinson (1985).

Figure 9 shows a geographic distribution of published $^{40}Ar/^{39}Ar$ and U/Pb ages from crystalline basement rocks north of the HSH area. Most of the small magmatic bodies in the surrounding hinterland of the Qaidam Basin are undated. However, based on previous geochronology, we can assume that they are either Mid-Palaeozoic or Mesozoic in the South Altyn basement exposed to the north of the HSH anticline, such as some of the already dated bodies (Delville et al., 2001; Sobel et al., 2001). Even though the source region for the dated HSH sediments has not remained constant with time because of strike-slip displacement along the Altyn fault, no change in the apparent detrital signal could be observed. This is particularly important for evaluating the source-sink relationship between the Palaeozoic belts in the North Altyn Mountains and the Qaidam Basin. Age groups from Eocene to Oligocene samples of the HSH First Valley show single-grain $^{40}Ar/^{39}Ar$ total fusion ages close to 450–500 Ma or even older, which are not known from the South Altyn Mountains, but from distinct regions northwest of the Xorkol basin within the North Altyn Mountains (Chen et al., 2003; cf. Fig. 9). We tentatively suggest an origin for these mica grains from the North Altyn Mountains. This is consistent with the observation that the South Altyn Mountains were uplifted during Early Miocene (e.g. Jolivet et al., 2001) successively forming a barrier and interrupting direct drainage from the North Altyn Mountains into the Qaidam Basin.

Although variable climatic conditions have been reconstructed for the Cenozoic (Wang et al., 1999), there is no shift in petrographical composition revealed in the sandstones from the HSH area (Fig. 7). During the Early Eocene, the Qaidam Basin subsided and subtropical conditions prevailed (Li, 1996). These conditions developed during deposition of the Xiaganchaigou Formation in the Middle Eocene when India-Asia collision (Harrison et al., 1992) and intracontinental convergence of India and Tibet started (Li, 1996) also involving the Qaidam block.

As for the composition of sandstones, our petrographic results plot into the recycled orogen field ($Q_t$-F-L), as expected because of the nature of the hinterland geology. Sediments in foreland basins are derived from nearby uplifting ranges and thus texturally and compositionally immature (Robinson et al., 2003) and therefore plot into the recycled orogen field in discrimination diagrams proposed by Dickinson and Suczek (1979). Even if hinterland geology changes through time, as long as the mineralogy of rocks in the hinterland stays the same, no changes can be observed in sandstone composition. In our study area, granitic bodies and basement gneisses have variable ages but had a similar mineralogical composition.

Liu et al. (2007) and Guo et al. (2006) did additional provenance studies on sandstones from the Third Valley section. They report a significant shift from the Xiaganchaigou Formation to the Shangganchaigou Formation shown in increased amounts of lithic clasts. In their study, they counted only 200 grains, which is virtually not sufficient in these rocks with minimum 20 percent matrix (Rieser et al., 2005). In such matrix-rich rocks, pseudomatrix could be formed by, e.g., decomposition of feldspar to clay minerals looking like lithic components.

The study of stable isotopes provided further indications of basin-scale tectonic and climatic changes. We sampled the southern limb of the anticline in the Third Valley and the northern limb in the Fifth Valley, which represents a “downward” extension of the Third Valley section (Fig. 8) with a probable, but small hiatus. An anoxic local depression in the Fifth Valley region could explain the difference in carbonate lithology of the two sections. A salinity gradient could also cause such differences (Zhang et al., 2003). The HSH Fifth Valley section further underlines the trend towards heavier carbon composition in the Xiaganchaigou Formation. One small negative isotopic excursion with an oxygen value of –7.5‰ might be due to, for example, cooler climatic conditions. A positive excursion is observed for both carbon and oxygen isotopes to –1.4 and –3.9‰, respectively at the lower end of the section. Further interpretation of these data remains open, as we have no further age constraint for this event or a comparative section within the Qaidam Basin.

If fine-grained carbonate rocks represent an expansion of the lake area and a deepening of the lake, significant changes in the lake level took place once every several thousand to more than two million years (Huang and Shao, 1993). Within the Third Valley section, which is characterised by synchronous positive $\delta^{13}C$ and $\delta^{18}O$ peaks, a cyclic pattern of 1 to 3 m.y. duration can be observed. Incomplete records and the availability of carbonate occurrences make it difficult to estimate the exact length of these and probably much shorter cycles within single carbonate beds. Excursions may be related

to arid to semi-arid conditions, which are also supported by the presence of anhydrite matrix in sandstones from boreholes in the Eocene Xiaganchaigou Formation (Rieser et al., 2005). Interestingly, Sun et al. (2009) report Palaeogene limestone and gypsum layers from the central Tarim Basin indicating, together with our data, widespread aridification. Repeated thin layers of coarse sands within the carbonates indicate short events of increased precipitation – either directly in the basin or in the adjacent mountains – which interrupt the general dry phase. The interfingering of these various deposits at the basin margin shows that the lake in the Qaidam Basin was not in a steady state but had a variable history with many shrinking and growing phases and local depressions.

The oxygen compositions show variable but progressively de-

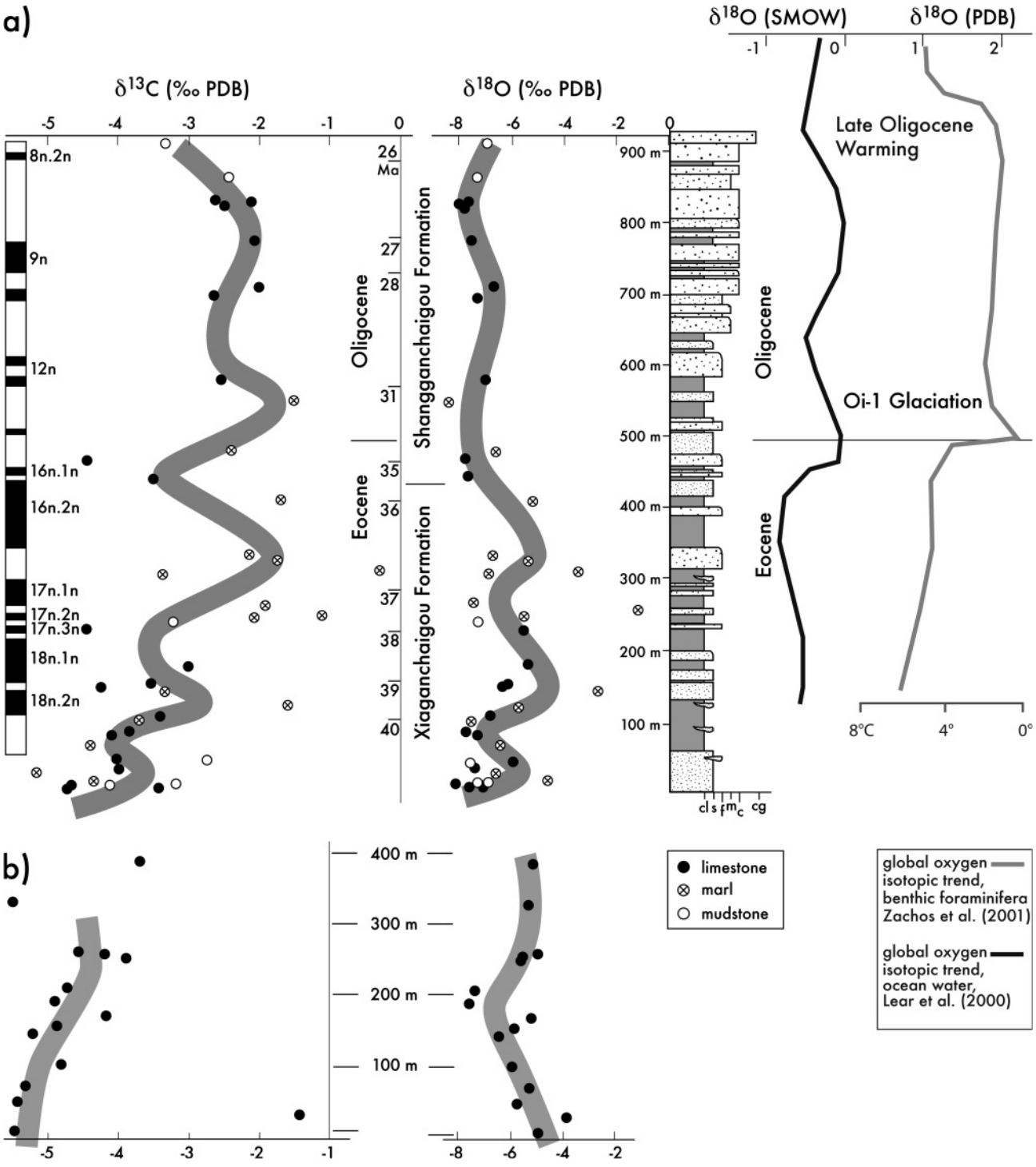


**Figure 8:** Stable isotope data for the Hongsanhan area. a) Stable isotope results for the Hongsanhan Third Valley are shown together with a recent magnetostratigraphy (Sun et al., 2005) and a simplified stratigraphic column (Ma, pers. comm. 2003) together with global oxygen curves (Lear et al., 2000; Zachos et al., 2001). b) Data from the Fifth Valley, which are believed to represent a downward continuation of the Third Valley section, but with a small missing interval.

creasing values from Eocene to Early Oligocene, i.e. from the Xiaganchaigou to the Shangganchaigou Formation (Fig. 8). As there are no major changes in the sedimentological record for this period, we conclude that rather environmental changes were responsible for the observed shift. We interpret the stable isotopic composition trend to indicate progressively cooler and/or wetter conditions, both factors causing lowering of the oxygen isotopic composition of carbonates. During Eocene to Oligocene, beside the global cooling trend (e.g. Lear et al., 2000; Zachos et al., 2001), the Qaidam Basin was characterised by northward drift (Wang et al., 1999). Therefore, the decreasing values of the oxygen isotopic composition are presumably related to cooling in higher latitudes or also higher altitudes due to convergence within the growing Tibetan plateau. Continental carbonates, in contrast to the marine ones, show generally lower isotopic values as temperature decreases (Hays and Grossman, 1991).

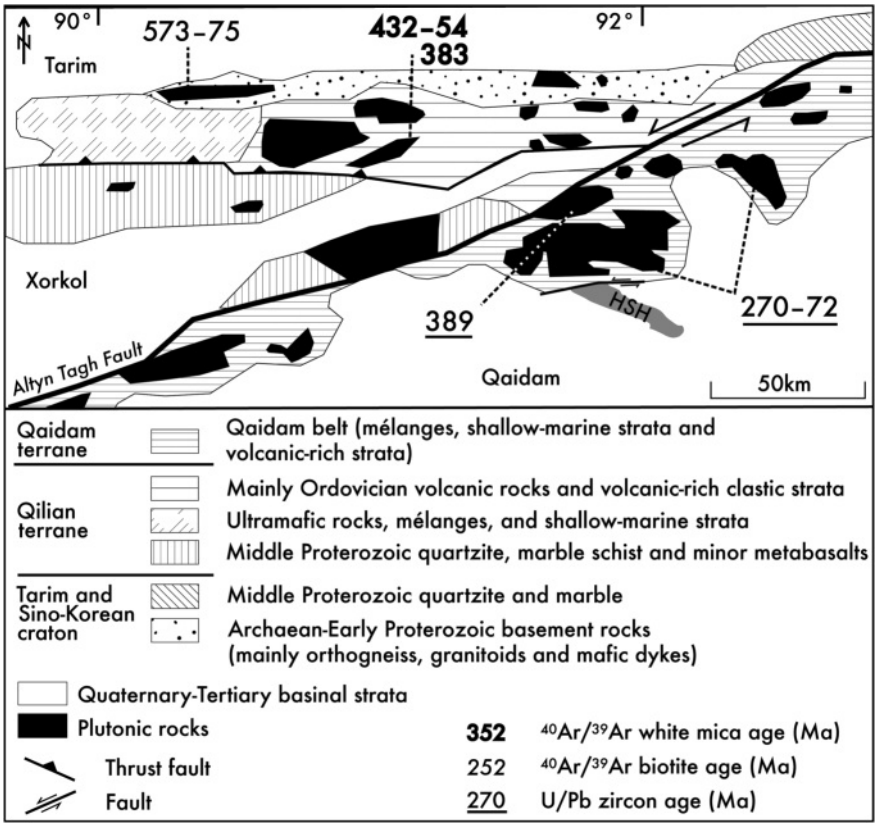


**Figure 9:** Geological map of the basement rocks in the Altyn Mountains north of the Hongsanhan anticline, showing published crystallization and cooling ages in Ma of magmatic units (Jolivet et al., 1999; Sobel et al., 2001; Gehrels et al., 2003a).

As the Eocene carbonates have a higher organic content than the Oligocene carbonates, the shift towards heavier isotopic composition observed for this interval cannot be related to increasing productivity. The sedimentary facies show increasing terrigenous input from the Xiaganchaigou to the Shangganchaigou Formation, which is also indicated by the change from limestone- to marl-dominated lithology (Fig. 8). A better explanation for the observed trend to higher $\delta^{13}C$ within the Oligocene, would be an increasing proportion of dissolved inorganic carbon transported by the inflowing waters or increasing aridity in the surroundings of the lake and thus a decreased contribution of soil derived $CO_2$ (Leng and Marshall, 2004; Bade et al., 2004).

The strongest uplift of the Himalaya-Tibet system was associated with a climate change (An et al., 2001) reflected in extremely variable $\delta^{13}C$ values starting with a positive excursion followed by a negative one at ca. 24 Ma in our record. Kent-Corson et al. (2009) found a similar change in many sections along the northern margin of the Tibetan plateau. Recently, Ritts et al. (2008) found early Miocene marine fossils at the northern margin of the Altyn Mountains, which are demonstrating the main period of surface uplift in the Altyn Mountains has occurred since that time.

## 6. Conclusion

Detailed investigation of the sedimentary succession exposed in the HSH anticline allows resolving the tectonic evolution and source-sink relationships between the northern Qaidam Basin and the South Altyn Mountains. Eocene coarse-grained clastic sediments record a proximal source although the $^{40}Ar/^{39}Ar$ age distribution of detrital white mica gives information on a distant source now exposed to the north of the Xorkol basin in the northwestern North Altyn Mountains. Together, coarse clastics and age patterns allow to demonstrate an Eocene juxtaposition of this specific source and the Qaidam basin fill now exposed whithin the HSH anticline, and a post-Eocene sinistral offset along the Datonggou and Altyn faults. The Late Eocene to Early Oligocene Xiaganchaigou and lowermost Shangganchaigou formations record lake-level high-stand and only distant sources excluding a basement high to the north of present-day HSH anticline at that time. A coarsening upward depositional cycle started at ca. 30–29 Ma and indicates onset of uplift of the South Altyn block. Modal analysis of samples in this study yields neither tectonic nor climatic information because mineralogy remained similar in the source area over time. Also the depositional area lies close to the basin margin, thus no transport effects are visible. Stable isotopes yield, despite the incomplete record, some climatic information that fit or depend on the tectonic situation at the northern margin of the Tibetan plateau.

## Acknowledgement

ABR gratefully acknowledges the Otto Ampferer award given

to her 2008 by the Austrian Geological Society, and its president, Christoph Spötl, for the proposal to write a manuscript on her research work. All authors, particularly ABR, would like to thank the colleagues in the field and at the institutes helping with preparation and measurements, especially Xiahong Ge, Gerti Friedl, Robert Handler and Ana-Voica Bojar. We gratefully acknowledge the careful, detailed and constructive review by David Schneider and also that of Christian Hager, and help by editors of the journal, Bernhard Grasemann and Hugh Rice.

## References

An, Z.S., Kutzbach, J.E., Prell, W.L. and Porter, S.C., 2001. Evolution of Asian monsoons and phased uplift of the Himalaya Tibetan plateau since late Miocene times. Nature, 411, 62-66.

Bade, D.B., Carpenter S.R., Cole, J.J., Hanson, P.C. and Hesslein, R.H., 2004. Controls of δ13C-DIC in lakes: geochemistry, lake metabolism, and morphometry. Limnology and Oceanography, 49/4, 1160-1172.

Brewer, I.D., Burbank, D.W. and Hodges, K., 2003. Modelling detrital cooling-age populations: insights from two Himalayan catchments. Basin Research, 15, 305-320.

Burbank, D.W., Blythe, A.E., Putkonen, J., Pratt-Sitaula, B., Gabet, E., Oskin, M., Barros, A. and Ojha, T.P., 2003. Decoupling of erosion and precipitation in the Himalayas. Nature, 426, 652-655.

Chen, X., Yin, A., Gehrels, G.E., Cowgill, E., Grove, M., Harrison, M. and Wang, X.-F., 2003. Two phases of Mesozoic north-south extension in the eastern Altyn Tagh range, northern Tibetan Plateau: Tectonics, 22, p. 1053, doi: 10.1029/2001TC001336.

Copeland, P. and Harrison, M., 1990. Episodic rapid uplift in the Himalaya revealed by $^{40}Ar/^{39}Ar$ analysis of detrital K-feldspar and muscovite, Bengal fan. Geology, 18, 354-357.

Delville, N., Arnaud, N., Montel, J.-M., Roger, F., Brunel, M., Tapponnier, P. and Sobel, E.R., 2001. Paleozoic to Cenozoic deformation along the Altyn-Tagh fault in the Altun Shan massif area, eastern Qilian Shan, northeastern Tibet, China. In: M.S. Hendrix and A.M. Davis (eds.), Paleozoic and Mesozoic Tectonic Evolution of Central Asia: From Continental Assembly to Intracontinental Deformation, Geological Society of America Memoir, 194, 269-292.

Dettman, D.L., Fang, X., Garzione, C.N. and Li, J., 2003. Uplift-driven climate change at 12 Ma: a long δ18O record from the NE margin of the Tibetan plateau. Earth and Planetary Science Letters, 214, 267-277.

Dickinson, WR., 1985. Interpreting provenance relations from detrital modes of sandstones. In: GG. Zuffa (ed.), Provenance of Arenites. Dordrecht: D. Reidel Publishing Company, pp. 333-361.

Dickinson, WR. and Suczek, CA., 1979. Plate tectonics and sandstone compositions. American Association of Petroleum Geologists Bulletin, 63(12), 2164-2182.

Fralick, P.W. and Kronberg, B.I., 1997. Geochemical discrimination of clastic sedimentary rock sources. Sedimentary Geology, 113, 111-124.

Garzione, C.N., Dettman, D.L. and Horton, B.K., 2004. Carbonate oxygen isotope paleoaltimetry: evaluating the effect of diagenesis on paleoelevation estimates for the Tibetan plateau. Palaeogeography Palaeoclimatology Palaeoecology, 212, 119-140.

Gehrels, G.E., Yin, A. and Wang, X.F., 2003a. Detrital-zircon geochronology of the northeastern Tibetan Plateau. Geological Society of America Bulletin, 115, 881-896.

Gehrels, G.E., Yin, A. and Wang, X.F., 2003b. Magmatic history of the northeastern Tibetan Plateau. Journal of Geophysical Research, 108, 2423, doi:10.1029/2002JB001876.

Genser, J., Neubauer, F., Liu, Y., Ge, X., Friedl, G. and Rieser, A., 2005. An active fault at the northern border of the Qaidam basin, China: Implications for extrusion models. Geologie Alpine Memoire H.S., 44, 66-67.

Gradstein, F.M., Ogg, J.G. and Smith, A., 2004. A Geologic Timescale 2004. Cambridge University Press, Cambridge, 610 pp.

Graham, S.A., Chamberlain, C.P., Yue, Y., Ritts, B.D., Hanson, A.D., Horton, T.W., Waldbauer, J.R., Poage, M.A. and Feng, X., 2005. Stable isotope records of Cenozoic climate and topography, Tibetan Plateau and Tarim Basin. American Journal of Science, 305, 101-118.

Guo, Z.T., Ruddiman, W.F., Hao, Q.Z., Wu, H.B., Qiao, Y.S., Zhu, R.X., Peng, S.Z., Wel, J.J., Yuan, B.Y. and Liu, T.S., 2002. Onset of Asian desertification by 22Myr ago inferred from loess deposits in China. Nature, 416, 159-163.

Guo, X., Liu, Y., Ge, X., Yuan, S., Sun, z., Pei, J. and Li, W., 2006. The Analyses of Cenozoic Sandstone Component in Hongsanhan No.1 Area and Its Tectonic Implications. Journal of Jilin University (Earth Science Edition), 36(2), 194-201.

Harrison, T.M., Copeland, P., Kidd, W.S.F. and Yin, A., 1992. Raising Tibet. Science, 255, 1663-1670.

Harrison, T.M., Célérier, J., Aikman, A.B., Hermann, J. and Heizler, M.T., 2009. Diffusion of $^{40}Ar$ in muscovite. Geochimica and Cosmochimica Acta, 73, 1039-1051.

Hays, P.D. and Grossman, E.L., 1991. Oxygen isotopes in meteoric calcite cements as indicators of continental paleoclimate. Geology, 19, 441-444.

Huang, Q. and Shao, H., 1993. Sedimentary characteristics and types of hydrocarbon source rocks in the Tertiary semiarid to arid lake basins of northwest China. Palaeogeography, Palaeoclimatology, Palaeoecology, 103, 33-43.

Johnsson, M.J., 1993. The system controlling the composition of clastic sediments. In: M.J. Johnsson, A. Basu (eds), Processes Controlling the Composition of Clastic Sediments. Geological Society of America Special Paper, 284, 1-19.

Jolivet, M., Roger, F., Arnaud, N., Brunel, M., Tapponnier, P. and Seward, D., 1999. Histoire de l'exhumation de l'Altun Shan: indications sur l'âge de la subduction du bloc du Tarim sous le système de l'Altun Thag (Nord Tibet). Comptes Rendus. Académie des Sciences Paris, 329, 749-755.

Jolivet, M., Brunel, M., Seward, D., Xu, Z., Yang, J. Roger, F., Tapponnier, P., Malavieille, J., Arnaud, N. and Wu, C., 2001. Mesozoic and Cenozoic tectonics of the northern edge of the Tibetan plateau: fission-track constraints. Tectonophysics, 343, 111-134.

Kent-Corson, M.L., Ritts, B. D., Zhuang, G., Bovet, P. M., Graham, S. A. and Chamberlain, C.P., 2009. Stable isotopic constraints on the tectonic, topographic, and climatic evolution of the northern margin of the Tibetan Plateau. Earth and Planetary Science Letters, 282, 158-166.

Lear, C.H., Elderfield, H. and Wilson, P.A., 2000. Cenozoic deep-sea temperatures and global ice volumes from Mg/Ca in benthic foraminiferal calcite. Science, 287, 269-272.

Leng, M.J. and Marshall, J.D., 2004. Palaeoclimate interpretation of stable isotope data from the lake sediment archives. Quaternary Science Reviews, 23(7-8), 811-831.

Li, T., 1996. The process and mechanism of the rise of the Qinghai-Tibet Plateau. Tectonophysics, 260, 45-53.

Liu, H., Liu, Y., Yuan, S., Ji, G. and Li, W., 2007. Provenance analysis of Eocene-Oligocene sandstones in the Hongsanhan area, northwestern Qaidam basin, Qinghai, China. Geological Bulletin of China, 26(1), 100-107.

McDougall, I. and Harrison, M.T., 1999. Geochronology and Thermochronology by the $^{40}Ar/^{39}Ar$ Method. 2nd ed, Oxford University Press, Oxford, 269 pp.

Meyer, B., Tapponnier, P., Bourjot, L., Métivier, F., Gaudemer, Y., Peltzer, G., Shunmin, G. and Zhitai, C., 1998. Crustal thickening in Gansu-Qinghai, lithospheric mantle subduction, and oblique, strike-slip controlled growth of the Tibet plateau. Geophysical Journal International, 135, 1-47.

Najman, Y., Pringle, M., Johnson, M.R.W., Robertson, A.H.F. and Wijbrans, J.R., 1997. Laser $^{40}Ar/^{39}Ar$ dating of single detrital muscovite grains from early foreland-basin sedimentary deposits in India: Implications for early Himalayan evolution. Geology, 25, 535-538.

Neubauer, F., Friedl, G., Genser, J., Handler, R., Mader, D. and Schneider, D., 2007a. Origin and tectonic evolution of Eastern Alps deduced from dating of detrital white mica: a review. Austrian Journal of Earth Sciences, 100 (Centennial Volume), 8-23.

Neubauer, F., Genser, J., Liu, Y. and Ren, S., 2007b. Basin-mountain coupling in transpressive settings: the North-Alpine front in Alps vs. the northeastern Tibet-Qaidam-Tarim system. Geophysical Research Abstracts, 9, EGU2007-A-09144.

Pettijohn, F.J., Potter, P.E. and Siever, R., 1987. Sand and Sandstone. Springer-Verlag, Berlin, 553 pp.

Ramstein, G., Fluteau, F., Besse, J. and Joussaume, S., 1997. Effect on orogeny, plate motion and land-sea distribution on Eurasian climate change over the past 30 million years. Nature, 386, 788-795.

Raymo, M.E. and Ruddiman, W.F., 1992. Tectonic forcing of late Cenozoic climate. Nature, 359, 117-122.

Rieser, A.B., Neubauer, F., Liu, Y. and Ge, X., 2005. Sandstone provenance of north-western sectors of the intracontinental Cenozoic Qaidam Basin, western China: tectonic vs. climatic control. Sedimentary Geology, 177, 1-18.

Rieser, A.B., Liu, Y., Genser, J., Neubauer, F., Handler, R., Friedl, G. and Ge, X., 2006. $^{40}Ar/^{39}Ar$ ages of detrital white mica constrain the Cenozoic development of the intracontinental Qaidam Basin, China. Geological Society of America Bulletin, 118, 1522-1534.

Rieser, A.B., Neubauer, F., Liu, Y., Genser, J., Handler, R., Ge, X. and Friedl, G., 2007. $^{40}Ar/^{39}Ar$ dating of detrital white mica as a complementary tool for provenance analysis: a case study from the Cenozoic Qaidam Basin (China). In: G. Nichols, E.A. Williams, C. Paola (eds.), Sedimentary Processes, Environments and Basins. International Association of Sedimentologists Special Publication, 38, 301-325.

Rieser, A.B., Bojar, A-V., Neubauer, F., Genser, J., Liu, Y., Ge, X. and Friedl, G., 2009. Monitoring Cenozoic climate evolution of northeastern Tibet: stable isotope constraints from the western Qaidam Basin, China. International Journal of Earth Sciences (Geologische Rundschau), 98. 1063-1075.

Ritts, B.D. and Biffi, U., 2001. Mesozoic northeast Qaidam basin: Response to contractional reactivation of the Qilian Shan, and implications for the extent of Mesozoic intracontinental deformation in central Asia. In: M.S. Hendrix and A.M. Davis (eds), Paleozoic and Mesozoic Tectonic Evolution of Central Asia: From Continental Assembly to Intracontinental Deformation, Geological Society of America, Memoir, 194, 293-316.

Ritts, B.D., Hanson, A.D., Zinniker, D. and Moldowan, J.M., 1999. Lower-Middle Jurassic nonmarine source rocks and petroleum systems of the Northern Qaidam Basin, Northwest China. American Association of Petroleum Geologists Bulletin, 83(12), 1980-2005.

Ritts, B.D., Yue, Y., Graham, S. A., Sobel, E.R., Abbink, O.A. and Stockli, D., 2008. From sea level to high elevation in 15 million years: Uplift history of the northern Tibetan Plateau margin in the Altun Shan. American Journal of Sciences, 308, 657-678.

Robinson, D.M., Dupont-Nivet, G., Gehrels, G.E. and Zhang, X., 2003. The Tula uplift, northwestern China: evidence for regional tectonism of the northern Tibetan Plateau during late Mesozoic-early Cenozoic time. Geological Society of America Bulletin, 115, 35-47.

Shi, Y., Yu, G., Liu, X., Li, B. and Yao, T., 2001. Reconstruction of the 30-40 ka BP enhanced Indian monsoon climate based on geological records from the Tibetan Plateau. Palaeogeography Palaeoclimatology Palaeoecology, 169, 69-83.

Sobel, E.R., Arnaud, N., Jolivet, M., Ritts, B.D. and Brunel, M., 2001. Jurassic to Cenozoic exhumation history of the Altyn Tagh range, NW China constrained by $^{40}Ar/^{39}Ar$ and apatite fission track thermochronology. In: M.S. Hendrix and G.A. Davis (eds.), Paleozoic and Mesozoic Tectonic Evolution of Central and Eastern Asia: from Continental Assembly to Intracontinental Deformation. Geological Society of America, Memoir 194, 1-15.

Song, T. and Wang, X., 1993. Structural styles and stratigraphic patterns of syndepositional faults in a contradictional setting: Examples from Qaidam Basin, NW China. American Association of Petroleum Geologists Bulletin, 77, 102-117.

Spicer, R.A., Harris, N.B.W., Widdowson, M., Herman, A.B., Guo, S., Valdes, P.J,. Wolfe, J.A. and Kelley, S., 2003. Constant elevation of southern Tibet over the past 15 million years. Nature, 421, 622-624.

Sun, J.,Zhang, Zh. and Zhang, L., 2009. New evidence on the age of the Taklimakan Desert. Geology, 37, 159–162.

Sun, X., Feng, X., Li, D., Yang, F., Qu, Y. and Wang, H., 1999. Cenozoic Ostracoda and palaeoenvironments of the northeastern Tarim Basin, western China. Palaeogeography Palaeoclimatology Palaeoecology, 148, 37-50.

Sun, X. and Wang, P., 2005. How old is the Asian monsoon system?– Palaeobotanical records from China. Palaeogeography Palaeoclimatology Palaeoecology, 222, 181-222.

Sun, Z., Yang, Z., Pei, J., Ge, X., Wang, X., Yang, T., Li, W. and Yuan, S., 2005. Magnetostratigraphy of Paleogene sediments from northern Qaidam Basin, China: implications for tectonic uplift and block rotation in northern Tibetan plateau. Earth Planetary Science Letters, 237, 635-646.

Tapponnier, P., Xu, Z., Roger, F., Meyer, B., Arnaud, N., Wittlinger, G. and Yang, J., 2001. Oblique stepwise rise and growth of the Tibet Plateau. Science, 294, 1671-1677.

Wang, E., Xu, F.Y. and Zhou, J.X., 2006. Eastward migration of the Qaidam basin and its implications for Cenozoic evolution of the Altyn Tagh fault and associated river systems. Geological Society of America Bulletin 118, 349-365.

Wang, J., Wang, J.Y., Liu, Z.C., Li, J.Q. and Xi, P., 1999. Cenozoic environmental evolution of the Qaidam Basin and its implications for the uplift of the Tibetan Plateau and the drying of central Asia. Palaeogeography Palaeoclimatology Palaeoecology, 152, 37-47.

Wang, J. and Zhang, M., 1999. Geological map of the Qaidam Basin 1:500'000. Jin Zhijun and Zhang Bingshan edn, Qinghai Oil Company and China Oil University, Beijing.

Willett, S.D. and Brandon, M.T., 2002. On steady states in mountain belts. Geology, 30, 175-178.

Yin, A., Manning, C.E., Lovera, O., Menold, C.A., Chen, X. and Gehrels, G.E., 2007. Early Paleozoic Tectonic and Thermomechanical Evolution of Ultrahigh-Pressure (UHP) Metamorphic Rocks in the Northern Tibetan Plateau, Northwest China. International Geology Review, 49, 681-716.

Yin, A., Dang, Y.Q., Wang, L.C., Jiang, W.M., Zhou, S.P., Chen, X.H., Gehrels, G.E. and McRivette, M.W., 2008a. Cenozoic tectonic evolution of Qaidam basin and its surrounding regions (Part 1): The southern Qilian Shan-Nan Shan thrust belt and northern Qaidam basin. Geological Society of America Bulletin, 120, 813-846.

Yin, A., Dang, Y.Q., Zhang, M., Chen, X.H. and McRivette, M.W., 2008b. Cenozoic tectonic evolution of the Qaidam basin and its surrounding regions (Part 3): Structural geology, sedimentation, and regional tectonic reconstruction. Geological Society of America Bulletin, 120, 847-876.

Zachos, J., Pagani, M., Sloan, L., Thomas, E. and Billups, K., 2001. Trends, Rhythms, and Aberrations in Global Climate 65 Ma to Present. Science, 292, 686-693.

Zhang, X., Hu, Y., Ma, L., Meng, Z., Duan, Y., Zhou, S. and Peng, D., 2003. Carbon isotope characteristics, origin and distribution of the natural gases from the Tertiary salty lacustrine facies in the west depression region in the Qaidam Basin. Science China (Series D), 46, 694-707.

Zhou, J., Xu, F., Wang, T., Cao, A. and Yin, Ch., 2006. Cenozoic deformation history of the Qaidam Basin, NW China: Results from cross-section restoration and implications for Qinghai–Tibet Plateau tectonics. Earth and Planetary Science Letters, 243, 195–210.

Zhu, L.D., Wang, C.S., Zheng, H.B., Xiang, F., Yi, H.S. and Liu, D.Z., 2006. Tectonic and sedimentary evolution of basins in the northeast of Qinghai-Tibet Plateau and their implication for the northward growth of the plateau. Palaeogeography Palaeoclimatology Palaeoecology, 241, Spec. Iss., 49-60.

Received: 15. June 2009
Accepted: 8. January 2010

Andrea Brigitte RIESER[1)*], Franz NEUBAUER[1)], Yongjiang LIU[2)] & Johann GENSER[1)]

[1)] Div. General Geology and Geodynamics, University of Salzburg, Hellbrunnerstrasse 34, 5020 Salzburg, Austria;

[2)] College of Earth Sciences, Jilin University, Changchun 130061, Jilin, China;

[*)] Corresponding author, andrea.rieser@nagra.ch